BIOLOGY OF REPRODUCTION (2016) **94**(4):93, 1–14
Published online before print 9 March 2016.
DOI 10.1095/biolreprod.115.133637

# Deletion of *Arid1a* in Reproductive Tract Mesenchymal Cells Reduces Fertility in Female Mice[1]

**Xiyin Wang,[3] Shikha Khatri,[4] Russell Broaddus,[5] Zhong Wang,[6] and Shannon M. Hawkins[2,3]**

[3]*Indiana University, Department of Obstetrics and Gynecology, Indianapolis, Indiana*
[4]*Baylor College of Medicine, Department of Obstetrics and Gynecology, Houston, Texas*
[5]*University of Texas MD Anderson Cancer Center, Department of Pathology, Houston, Texas*
[6]*University of Michigan, Department of Cardiac Surgery, Ann Arbor, Michigan*

## ABSTRACT

**Women with endometriosis can suffer from decreased fecundity or complete infertility via abnormal oocyte function or impaired placental-uterine interactions required for normal pregnancy establishment and maintenance. Although AT-rich interactive domain 1A (SWI-like) (ARID1A) is a putative tumor suppressor in human endometrial cancers and endometriosis-associated ovarian cancers, little is known about its role in normal uterine function. To study the potential function of ARID1A in the female reproductive tract, we generated mice with a conditional knockout of *Arid1a* using anti-Müllerian hormone receptor 2-*Cre*. Female *Arid1a* conditional knockout mice exhibited a progressive decrease in number of pups per litter, with a precipitous decline after the second litter. We observed no tumors in virgin mice, although one knockout mouse developed a uterine tumor after pregnancy. Unstimulated virgin female knockout mice showed normal oviductal, ovarian, and uterine histology. Uteri of *Arid1a* knockout mice showed a normal decidualization response and appropriate responses to estradiol and progesterone stimulation. In vitro studies using primary cultures of human endometrial stromal fibroblasts revealed that small interfering RNA knockdown of *ARID1A* did not affect decidualization in vitro. Timed pregnancy studies revealed the significant resorption of embryos at Embryonic Day 16.5 in knockout mice in the third pregnancy. In addition to evidence of implantation site hemorrhage, pregnant *Arid1a* knockout mice showed abnormal placental morphology. These results suggest that *Arid1a* supports successful pregnancy through its role in placental function.**

*ARID1A, female reproductive tract, fertility, genetically engineered mouse models, placenta, tumor suppressor, uterus*

## INTRODUCTION

The AT-rich interactive domain 1A (SWI-like) (*Arid1a*) gene encodes a large nuclear protein that is a key subunit of the multiprotein SWI/SNF chromatin-remodeling complex that is present in all eukaryotes. The SWI/SNF complex regulates gene expression for a variety of cellular processes, including differentiation, proliferation, DNA repair, and tumor suppression. The complex uses ATP as energy to mobilize nucleosomes, thereby modulating the accessibility of promoters to transcriptional activation or repression [1, 2].

Loss of ARID1A has been discovered in many human cancers, including renal cell carcinoma, gastric carcinoma, bladder tumors, pancreatic cancer, colon cancer, breast cancer, endometriosis-associated ovarian carcinomas, and uterine endometrioid carcinomas [3–20]. Considering gynecological cancer types, *ARID1A* mutation is a driver mutation for endometrial cancer, giving an advantage to epithelial cell growth in vitro [19]. Evidence from ovarian cancer cell lines supports the idea that ARID1A functions as a tumor suppressor by binding to tumor protein p53 (TP53) and regulating cyclin-dependent kinase inhibitor 1A (CDKN1A) [20].

Although ARID1A-inactivating mutations occur in a wide variety of tumors of the female reproductive tract in humans, inactivation of ARID1A alone is insufficient for tumor initiation in the female reproductive tract of mice [21, 22]. Studies using adenovirus-driven *Cre* to delete *Arid1a* in the ovarian surface epithelium showed that deletion of *Arid1a* alone is not sufficient for ovarian cancer formation. Rather, female reproductive tract tumor formation required additional mutation in phosphatase and tensin homolog (*Pten*) or phosphatidylinositol-4,5-bisphosphate 3-kinase, catalytic subunit alpha (*Pik3ca*) [22, 23]. Studies using progesterone receptor (*Pgr*)-driven *Cre* to delete *Arid1a* in the uterus showed that deletion of *Arid1a* alone is not sufficient for endometrial cancer formation [21]. Although these studies suggest the potential cooperation between mutation of *Arid1a* and other tumor suppressors in tumorigenesis, little is known about the role of ARID1A in the normal female reproductive tract.

ARID1A is essential for mammalian development because deletion of *Arid1a* in traditional knockout mice causes embryonic lethality resulting from defects in mesoderm

[1]This work was supported by The Liz Tilberis Scholarship Ovarian Cancer Research Fund through the Estate of Agatha Fort and an MD Anderson Cancer Center SPORE in Ovarian Cancer Developmental Research Project Award (grant number P50-CA83639) to S.M.H., and funding from the National Institutes of Health (grant number HL109054) to W.Z. The Pathology and Histology Core and the Genetically Engineered Mouse Core at Baylor College of Medicine also supported this project with funding from the National Institutes of Health (NCI P30-CA125123). This work was supported by the *Eunice Kennedy Shriver* National Institute of Child Health and Human Development/National Institutes of Health through Cooperative Agreements U54HD028934 (to the University of Virginia Center for Research in Reproduction Ligand Assay and Analysis Core, Charlottesville, VA) as part of the Specialized Cooperative Centers Program in Reproduction and Infertility Research. Presented in part at the 45th Annual Meeting of the Society for the Study of Reproduction, 12–15 August 2012, State College, Pennsylvania.
[2]Correspondence: Shannon M. Hawkins, Indiana University School of Medicine, Department of Obstetrics and Gynecology, 550 N. University Blvd, UH2440, Indianapolis, IN 46202. E-mail: shhawkin@iu.edu

Received: 18 August 2015.
First decision: 17 September 2015.
Accepted: 3 March 2016.

eISSN: 1529-7268 http://www.biolreprod.org
ISSN: 0006-3363

development and embryonic stem cell self-renewal, differentiation, and cell lineage decisions [24]. To overcome this early defect and study the global roles of ARID1A in mammals, others have developed *Arid1a* floxed alleles [24] for the conditional ablation of *Arid1a*, which has shed light on the role of *Arid1a* in regulating key genes in cardiac development [25]. Recently, we showed that deletion of *Arid1a* from the *Pgr*-positive cells of the uterus resulted in complete sterility with defective embryo implantation and uterine decidualization. The underlying mechanism of this sterility phenotype was from the effects of ARID1A and PGR on expression of Kruppel-like factor 15 (*Klf15*) and on uterine epithelial cell proliferation [21]. To study the broader role of *Arid1a* in the female reproductive tract, we used the anti-Müllerian hormone receptor 2 (*Amhr2*)-*Cre* mouse model [26], which has *Cre* recombinase inserted into the *Amhr2* gene. Therefore, *Cre* is expressed in cells that express *Amhr2*, which include mesenchymal cells of the uterus such as uterine stromal and myometrial cells, oviductal cells, and somatic cells of the ovary such as surface epithelial and granulosa cells [26–30]. Expression of *Amhr2* is detectable as early as the 8-cell stage [31], and its expression in the gonad is present beginning at Embryonic Day 12.5 [27]. *Amhr2-Cre* mice have been successfully used to study the roles of many genes in female reproduction and cancer, including vascular endothelial growth factor a (*Vegfa*) [32], *miR-34c* [33], signal transducer and activator of transcription 3 (*Stat3*) [34], transforming growth factor beta receptor 1 (*Tgfbr1*) [35], transformation protein related protein 53 (*Trp53*) [36–38], *Pten* [28, 36, 37, 39–42], Kirsten rat sarcoma viral oncogene homolog (*Kras*) [28, 36, 37, 43], beta catenin 1 (*Ctnnb1*) [29, 39, 44–47], tuberous sclerosis 1 (*Tsc1*) [48, 49], smoothened, frizzled class receptor (*Smo*) [50–53], adenomatous polyposis coli (*Apc*) [54], wingless-type MMTV integration site family, member 4 (*Wnt4*) [55], breast cancer 1, early onset (*Brac1*) [38], *Dicer1* [42, 56–58], nuclear receptor subfamily 2, group F, member 2 (*Nr2f2*) [59], splicing factor 1 (*Sf1*) [60], activins [61], follistatin (*Fst*) [62], and Smads [63, 64]. Here, using *Amhr2-Cre* mice, we show that deletion of *Arid1a* leads to a progressive loss of fertility via placental disruption.

## MATERIALS AND METHODS

### *Generation and Genotyping of* Arid1a *Conditional Knockout Mice*

*Arid1a* conditional allele ($Arid1a^{flox/flox}$) mice have been described previously [24] and were maintained in a C57BL/6J; 129S5/Brd mixed hybrid background. $Arid1a^{flox/flox}$ mice were bred to $Amhr2^{cre/+}$ mice [26] to generate $Arid1a^{flox/+}$;$Amhr2^{cre/+}$ mice. $Arid1a^{flox/+}$;$Amhr2^{cre/+}$ male mice were crossed to $Arid1a^{flox/flox}$ female mice to generate final breeder pairs of $Arid1a^{flox/flox}$;$Amhr2^{cre/+}$ male mice and $Arid1a^{flox/flox}$ female mice. These final breeders were used to generate the experimental female mice: $Arid1a^{flox/flox}$;$Amhr2^{cre/+}$ mice (termed *Arid1a* conditional knockout [cKO] mice) and $Arid1a^{flox/flox}$ mice (termed control mice) (Supplemental Fig. S1A; Supplemental Data are available online at www.biolreprod.org). $Arid1a^{flox/-}$;$Amhr2^{cre/+}$ mice were not generated because previous studies show that *Arid1a* heterozygosity ($Arid1a^{+/-}$) leads to embryonic lethality in mice, similar to homozygous deletion [24]. All mice were maintained in accordance with the National Institutes of Health Guide for the Care and Use of Laboratory Animals under an approved protocol. The Baylor College of Medicine Genetically Engineered Mouse Core performed rederivation and initial breeding. Mice were genotyped at 12–14 days of postnatal life from tail biopsies by PCR analyses using specific primers [22, 65] (Supplemental Table S1 and Supplemental Fig. S1B). For the *Arid1a* floxed allele, the following conditions were used with *Arid1a* forward and reverse primers: 2 min at 50°C, 10 min at 95°C, followed by 40 cycles of 15 sec at 95°C (denaturation), 45 sec at 59°C (annealing), and 45 sec at 72°C (extension). For the *Cre* allele, the following conditions were used with *Amhr2-Cre* forward and reverse primers: 2 min at 50°C, 10 min at 95°C, followed by 40 cycles of 15 sec at 95°C (denaturation), 45 sec at 60°C (annealing), and 45 sec at 72°C (extension).

### *Fertility Analysis and Studies Involving Parous Uteri*

To evaluate reproductive performance, 6-wk-old female control and *Arid1a* cKO mice were bred to wild-type C57BL/6J;129S5Brd hybrid male mice of proven fertility. The numbers of litters and pups were recorded over a 6-mo period. After the 6-mo fertility studies were completed, female mice were rested for 2 mo. Mice were then euthanized, and the parous uteri were fixed for histology.

### *Tissue Collection, Histological Analysis, and Timed Pregnancy*

At times listed in experimental design below, mice were euthanized; reproductive organs were excised and fixed for histology or snap frozen for RNA or protein isolation. Uteri, implantation sites, and placentas were fixed in 4% paraformaldehyde (Sigma), and ovaries were fixed in 10% neutral buffered formalin (EMD Millipore). The Baylor College of Medicine Human Tissue Acquisition and Pathology Core performed tissue processing and paraffin embedding. Sections were cut at 5 μm and stained with hematoxylin (VWR) and eosin (VWR) or periodic acid-Schiff (Sigma) using standard techniques. Tissue and serum samples from timed pregnancies were obtained by mating *Arid1a* cKO and control female mice with intact wild-type C57BL/6;129S5/Brd hybrid male mice. The morning that the vaginal plug was observed was designated as 0.5 days postcoitus (dpc). Mice were euthanized on Day 4.5, 8.5, 9.5, or 16.5 of pregnancy, and the number of implantation sites was counted.

### *Steroid Hormone Treatment and Artificial Induction of Decidualization*

Beginning at 6 wk of age, *Arid1a* cKO and control female mice underwent bilateral ovariectomy followed by rest for 2 wk. For steroid hormone responsive studies, mice were treated with either 1 mg progesterone (P4) for 6 h [66, 67] or 100 ng 17β-estradiol (E2) for three consecutive days [68]. Sesame oil was used as a vehicle control (all reagents from Sigma).

The artificial induction of uterine decidualization has been previously described [69]. Briefly, 2 wk after ovariectomy, *Arid1a* cKO and control female mice were primed with 100 ng E2 per day for 3 days, followed by 2 days of rest and then 3 daily injections of 1 mg P4 and 6.7 ng E2. Six hours after the last injection, the left uterine horn was stimulated by a scratch with a burred needle. Daily injections of 1 mg P4 and 6.7 ng E2 were continued for 5 days. Mice were euthanized on Day 5. The uteri were dissected, weighed, and fixed in 4% paraformaldehyde.

### *Superovulation*

Superovulation experiments were carried out as previously described [70]. At 21 days of age, *Arid1a* cKO and control female mice were injected intraperitoneally with 5 IU equine chorionic gonadotropin (Calbiochem) for 46 h, followed by intraperitoneal injection with 5 IU human chorionic gonadotropin (Novarel; Ferring Pharmaceuticals). Mice were then bred to wild-type male mice with proven fertility. Mice were dissected at 4.5 dpc.

### *Serum Analysis*

Adult *Arid1a* cKO and control female mice were anesthetized by isoflurane inhalation (Abbott Laboratories), and blood was collected in microtainer tubes (Becton Dickinson) by closed cardiac puncture. Serum was separated by centrifugation and stored at −20°C until use. The University of Virginia Ligand Assay and Analysis Core performed measurements of follicle stimulating hormone (FSH), luteinizing hormone (LH), anti-Müllerian hormone (AMH), E2, and P4 levels.

### *Immunohistochemical Staining*

Three sections from each of three independent control and *Arid1a* cKO uteri or ovary were analyzed in parallel. Paraffin-embedded tissues were cut at 5 μm, mounted on silane-coated slides, deparaffinized, rehydrated in graded alcohol series, and boiled in citrate buffer, pH 6.0 (Abcam) prior to blocking with 10% normal goat serum and incubating in primary antibody diluted in 10% normal goat serum (Vector Laboratories) in phosphate-buffered saline (PBS), pH 7.5 (Life Technologies, Inc.) overnight at 4°C. Primary antibodies and conditions are listed in Supplemental Table S2. Sections were washed with

PBS and incubated with the appropriate species-specific horseradish peroxidase-conjugated secondary antibody (2 μg/ml; Vector Laboratories) for 1 h at room temperature. Immunoreactivity was detected using the Vectastain Elite DAB kit (Vector Laboratories). Sections were then briefly counterstained with hematoxylin, dehydrated, and mounted. Slides were analyzed by light microscopy.

### RNA Isolation and Real-Time Quantitative PCR Analysis

Total RNA was extracted using the mirVana microRNA isolation kit (Life Technologies, Inc.). After nucleic acid quantification on a NanoDrop ND-1000 (Thermo Scientific), RNA was treated with Turbo DNAse (Life Technologies, Inc.) according to the manufacturer's protocol. DNAse-treated RNA (1000 ng) was reverse transcribed in a 50 μl reaction using 250 U Superscript III reverse transcriptase (Life Technologies, Inc.) with random primers (Life Technologies, Inc.). Samples were diluted to 100 μl, and 2 μl was used for each quantitative PCR (qPCR) reaction. Real-time qPCR was performed on the ABI StepOnePlus using either predesigned TaqMan Gene Expression Assays (Life Technologies, Inc.) or custom primers designed using Primer Express software (Life Technologies, Inc.) for SYBR green (Supplemental Table S1). Levels of mouse ribosomal protein L13a (*Rpl13a*) or *18s* were used as endogenous controls for mouse uterus samples as expression of *Rpl13a* and *18s* were shown not to change in response to steroid hormone stimulation [66, 71]. Levels of glyceraldehyde-3-phosphate dehydrogenase (*Gapdh*) were used for placenta as previous studies have shown this is a reasonable endogenous control for mouse placenta [72, 73]. Levels of human ribosomal protein L19 (*RPL19*) were used as endogenous controls for human samples [66, 74–76]. TaqMan PCR was performed using TaqMan universal PCR master mix (Life Technologies, Inc.), and PCR with custom primers was performed using SYBR Green PCR master mix (Life Technologies, Inc.) in a 10-μl reaction. The reaction conditions were as follows: 2 min at 50°C, 10 min at 95°C, followed by 40 cycles of 15 sec at 95°C (denaturation) and 1 min at 60°C (annealing/extension). Each sample was analyzed in duplicate or triplicate, and a nontemplate control (nuclease-free water) was included on each plate for each primer-probe set. All custom primers had an efficiency of 85%–110%. All SYBR green runs had dissociation curves to predict potential primer-dimers. The relative quantity of transcript was calculated using the $2^{-\Delta\Delta Ct}$ method [77].

### Institutional Review Board Approval, Collection of Human Tissues, Creation of Primary Cultures, and Transfection of Cells

All human tissues were collected under Baylor College of Medicine Institutional Review Board approval with written informed consent, and cultures were created as described previously [76]. Cells were transfected and underwent in vitro decidualization as described previously [78]. Briefly, 2 days before induction of in vitro decidualization, cells in 6-well plates were treated with Dulbecco-modified Eagle medium/F12 with 2% charcoal-stripped fetal bovine serum (Life Technologies, Inc.) containing 5 μl RNAiMax (Life Technologies, Inc.) with 100 nM of either nontargeting small interfering RNA (siNT) (ON-TARGETplus Non-targeting Control Pool, Thermo Scientific) or small interfering RNA targeting *ARID1A* (siARID1A) (ON-TARGETplus Human *ARID1A* small interfering RNA, Thermo Scientific) dissolved in Opti-MEM (Invitrogen). On the day of decidualization induction, which was designated as Day 0, an aliquot of cells for each treatment (siNT or siARID1A) was collected, and the remaining cells were treated with decidual medium containing $10^{-8}$ M E2, $10^{-6}$ M medroxyprogesterone acetate, and 50 μM 8-bromocyclic AMP in Opti-MEM with 2% charcoal-stripped fetal bovine serum and 1% antibiotic-antimycotic (Invitrogen) as described previously [76]. The medium was changed using freshly prepared decidual medium on Days 2 and 4. On Day 6, cells were washed with PBS, scraped from plates, and harvested in lysis buffer for RNA isolation as described above.

### Statistical Analysis

Student *t*-test or two-way ANOVA with post hoc tests were performed using GraphPad Prism software version 6.0c. For the timed pregnancy study, chi-square analysis was performed. Data are presented as mean ± standard error of the mean, and $P < 0.05$ was considered statistically significant.

## RESULTS

### Arid1a *cKO Mice Did Not Develop Ovarian Cancer*

To generate female mice lacking expression of *Arid1a* in the reproductive tract, $Arid1a^{flox/flox}$ mice [24] and $Amhr2^{cre/+}$ mice [26] that express *Cre* recombinase under the control of the *Amhr2* promoter were obtained. Supplemental Figure S1A shows the detailed breeding strategy to generate $Arid1a^{flox/flox}$; $Amhr2^{cre/+}$ mice (termed *Arid1a* cKO mice) and $Arid1a^{flox/flox}$ mice (termed control mice). Previous studies show that similar strategies are successful in disrupting ARID1A function [21, 24, 25].

We found that female *Arid1a* cKO and control mice were born healthy. To confirm tissue-specific recombination and ablation of *Arid1a*, we performed qPCR and immunohistochemical staining on tissues from virgin 12-wk-old female mice. Quantitative PCR revealed a 1.58-fold decrease ($n = 8$, Student *t*-test, $P < 0.05$) in *Arid1a* in whole uteri of adult *Arid1a* cKO mice compared with control mice (Fig. 1A). This sizeable but incomplete ablation of *Arid1a* in the uterus may be due to the lack of *Arid1a* deletion in the uterine epithelium. Next, we used immunohistochemistry to examine the cell type-specific expression of ARID1A. In uteri from virgin control female mice, ARID1A was expressed in the nuclei of uterine luminal and glandular epithelial cells, uterine stromal cells, and myometrial cells (Fig. 1, B and C). In uteri from virgin *Arid1a* cKO female mice, there was a lack of ARID1A staining in the uterine stroma but observable staining in uterine luminal and glandular epithelial cells (Fig. 1, D and E). This cell type-specific depletion of ARID1A in the uterus is consistent with previous work showing AMHR2 expression in uterine stromal cells [30]. Thus, as expected, ablation of *Arid1a* in the uterus of cKO mice was cell type specific.

*Amhr2-Cre* should lead to recombination in somatic cells of the ovary, including granulosa cells and ovarian surface epithelial cells [26, 28]. In virgin 12-wk-old female control mice, ARID1A was detected in ovarian theca cells, in somatic cells of ovarian follicles at all stages of follicular development, and in ovarian surface epithelial cells (Supplemental Fig. S2, A and B). In unstimulated virgin female *Arid1a* cKO mice, there was decreased ARID1A staining in granulosa cells and ovarian surface epithelial cells (Supplemental Fig. S2, C and D). Previous work had shown that deletion of *Pten* and *Dicer* using *Amhr2-Cre* lead to high-grade serous ovarian cancers that arose in the oviduct [42]. ARID1A was detected in nuclei of the columnar epithelium of the oviduct in both virgin control (Supplemental Fig. S2, E and F) and *Arid1a* cKO mice (Supplemental Fig. S2, G and H).

Because loss of ARID1A in epithelial cells is a common feature of human endometriosis-associated ovarian cancers [9, 11], we performed long-term survival studies with virgin female control and *Arid1a* cKO mice ($n = 20$ per genotype). We observed no differences ($P = 0.575$) between genotypes in body weight over time (Supplemental Fig. S3). No control or *Arid1a* cKO mice were euthanized due to disease. Furthermore, at 1 yr of age, both virgin control and virgin *Arid1a* cKO mice had normal reproductive tract histology (data not shown). These results indicate that virgin female *Arid1a* cKO mice did not develop ovarian cancer.

### Arid1a *cKO Mice Exhibited a Progressive Decline in Fertility*

To evaluate fertility, female control and *Arid1a* cKO mice ($n = 9$ per genotype) were housed with wild-type males for 6 mo. *Arid1a* cKO mice were less fertile than control mice, with

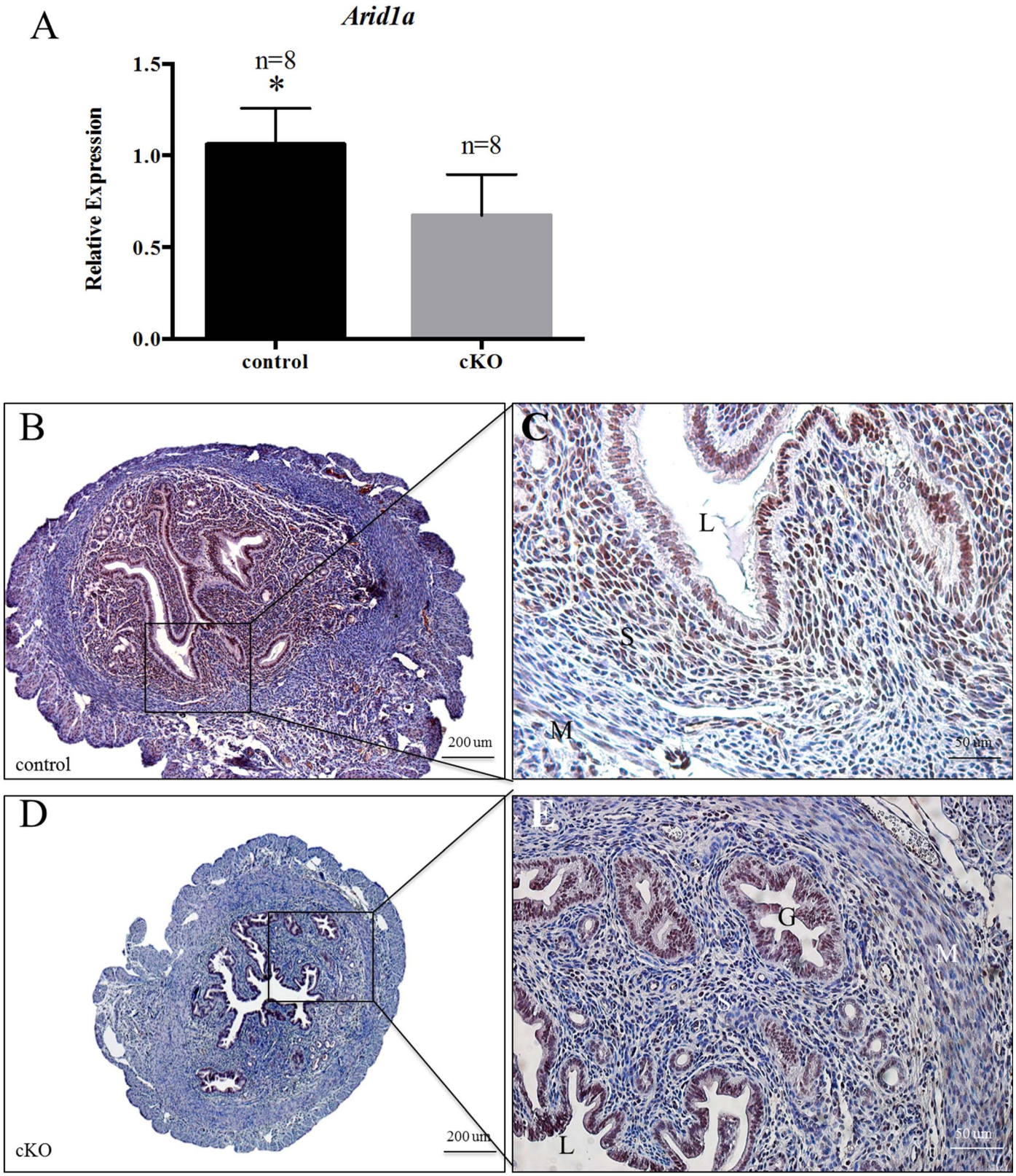


FIG. 1. Deletion of *Arid1a* in the uterine stroma of *Arid1a* cKO mice. Quantitative PCR showed that uteri from virgin 12-wk-old cKO mice showed decreased expression of *Arid1a* compared with control mice (**A**). Comparison of immunohistochemical staining for ARID1A in virgin 12-wk-old control (**B**, **C**) and cKO (**D**, **E**) mice. Statistical significance (*$P < 0.05$) was calculated by Student *t*-test. Relative expression of *Arid1a* to *18s*; G, glandular epithelium; L, lumen; M, myometrium; S, uterine stroma. Bars = 200 μm (**B**, **D**) and 50 μm.

significantly fewer pups per litter (Student *t*-test, $P < 0.05$; Fig. 2A) and significantly fewer litters per month (cKO: 0.7 ± 0.3; control: 1.1 ± 0.1; Student *t*-test, $P < 0.05$). Litter size was significantly smaller in *Arid1a* cKO mice (4.0 ± 1.9 pups per litter) compared with control female mice (7.5 ± 1.5 pups per litter; Student *t*-test, $P < 0.001$). Furthermore, this subfertility

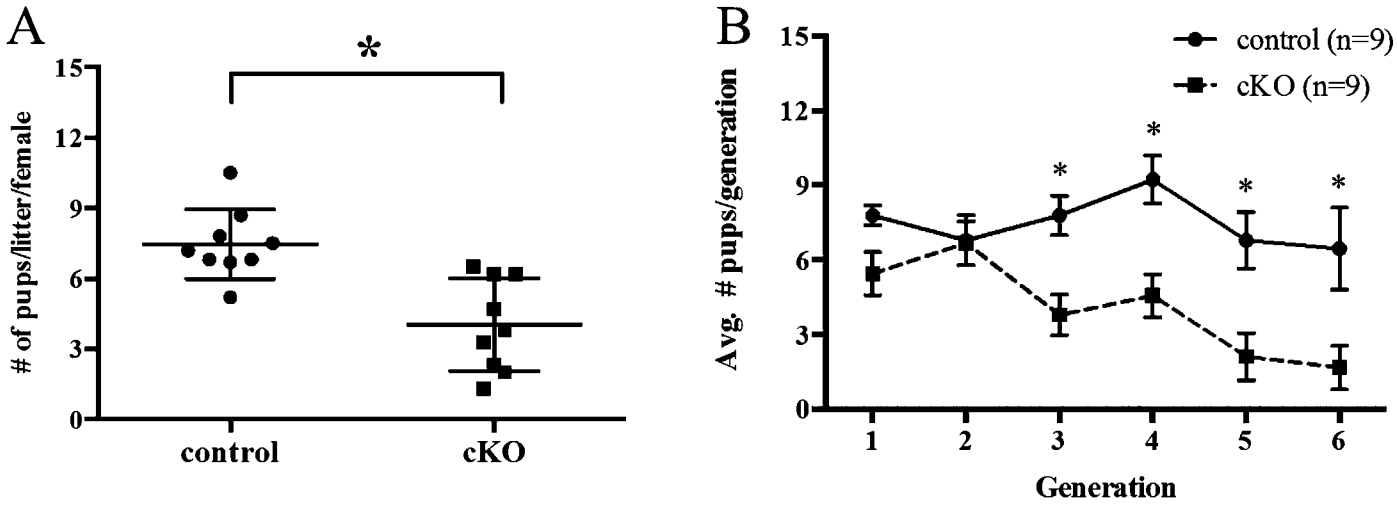


FIG. 2. *Arid1a* cKO mice exhibited progressive subfertility. The reproductive ability of mice was tracked over a 6-mo breeding period. *Arid1a* cKO mice had fewer pups per litter than control mice (**A**). Conditional knockout mice showed a progressive decline in fertility as evidenced by a lower total number of pups per generation (**B**). Statistical significance (*$P < 0.05$) was calculated by Student *t*-test (**A**) or two-way ANOVA (**B**).

worsened over time. Although the total number of pups per generation was lower for *Arid1a* cKO mice than for control mice across all generations (two-way ANOVA, $P = 0.0064$), there was a progressive decline after the second pregnancy (Fig. 2B). In addition, three out of nine *Arid1a* cKO mice were infertile by 5 mo of age, whereas all control mice were still fertile at this age, thus demonstrating the importance of *Arid1a* in pregnancy.

### Arid1a *cKO Mice Had Low Penetrance of Uterine Tumors after Pregnancy*

After the fertility experiments, parous female mice were dissected at 8 mo of age to evaluate the reproductive tract. Control mice had grossly normal reproductive tracts, with no uterine or ovarian tumors (Supplemental Fig. S4A and data not shown). Parous control mice also had normal uterine histology, with similar ARID1A expression as virgin female mice (Supplemental Fig. S4B). Parous *Arid1a* cKO mice had normal uterine histology, with similar ARID1A expression as virgin female mice (Supplemental Fig. S4D). However, of the nine parous *Arid1a* cKO mice, one mouse had a uterine tumor, although both ovaries, both oviducts, and the opposite uterine horn in this mouse were grossly and histologically normal (Supplemental Fig. S4, A and D, and data not shown). Histological analysis showed that the tumor was a benign smooth muscle tumor with complete ablation of ARID1A in both the uterine stroma and epithelium (Supplemental Fig. S4C). In the normal horn, ARID1A expression was detected in the nuclei of glandular and luminal epithelial cells (Supplemental Fig. S4D), similar to its expression in virgin *Arid1a* cKO uteri. Overall, other than one benign uterine tumor, parous *Arid1a* cKO and virgin *Arid1a* cKO female mice had normal histology of female reproductive tract with no difference in ARID1A expression or localization.

### *Virgin* Arid1a *cKO Mice Had Normal Reproductive Tracts, Gonadotropin Levels, and Steroid Hormone Responses*

*Amhr2-Cre* deletes the target allele in mesenchymal cells of the uterus, oviduct, and ovary, all of which may contribute to the subfertility phenotype observed in *Arid1a* cKO mice. Previous in vivo models of subfertility with *Amhr2-Cre* have shown defects in virgin or primigravid reproductive tract such as *Stat3* [34], *Kras* [37], *Pten* [41], *Wnt4* [55], and *Nr2f2* [59]. Therefore, we undertook a systematic approach to examine the contribution of *Arid1a* deletion in each organ system in virgin female mice.

To characterize the uterus of *Arid1a* cKO mice, virgin mice were euthanized at 12 wk of age. Gross observation showed that the uterus of *Arid1a* cKO mice was smaller than that of control mice (Fig. 3A), and measurement of uterine weight revealed significantly lighter uteri in *Arid1a* cKO mice than in control mice ($n = 8$, Student *t*-test, $P < 0.05$; Fig. 3B). Furthermore, *Arid1a* cKO mice had significantly more uterine glands per $mm^2$ of surface area encapsulated by the myometrium than control mice ($n = 4$, $P < 0.05$; Fig. 3C), as well as a 2-fold increase in levels of *Foxa2* ($n > 4$, $P < 0.05$; Fig. 3D), a marker of glandular epithelium [79]. Previous work shows a critical role of *Tgfbr1* in uterine smooth muscle development [80, 81], but we observed no differences between genotypes in levels of *Tgfbr1* (data not shown). Both cyclin D1 (*CCND1*) and B-cell CLL/lymphoma 2 (*BCL2*) are regulated by ARID1A in human non-small cell lung cancer [82]. We further investigated molecular changes by measuring levels of the cell cycle pathway- and apoptosis-related genes (*Ccnd1*) and (*Bcl2*) in virgin uteri. We found a 1.4-fold ($n > 4$, $P < 0.05$) and 2.2-fold ($n > 4$, $P < 0.05$) increase in *Ccnd1* and *Bcl2* levels in unstimulated virgin adult *Arid1a* cKO uteri, respectively (Fig. 3, E and F). However, there was no difference in caspase-3 or Ki-67 staining in unstimulated virgin *Arid1a* cKO and control uteri (data not shown).

Histological analysis demonstrated that at 4, 12, and 52 wk of age, the morphology and histology of virgin ovaries was similar between control and *Arid1a* cKO mice (Supplemental Fig. S5, A–F). When superovulation was induced in immature mice ($n = 23$ per genotype), virgin control and *Arid1a* cKO mice showed similar histology and numbers of corpora lutea (Supplemental Fig. S5, G–L). Furthermore, when we quantified serum AMH levels as a measure of ovarian reserve, we found no significant difference between virgin control (15.64 ± 2.321 ng/ml, $n = 9$) and virgin *Arid1a* cKO (12.93 ± 2.268 ng/ml, $n = 8$; Student *t*-test, $P = 0.179$) mice.

To examine gonadotropin hormone levels, we measured FSH and LH serum hormone levels of unstimulated, randomly cycling adult *Arid1a* cKO and control mice. We observed no

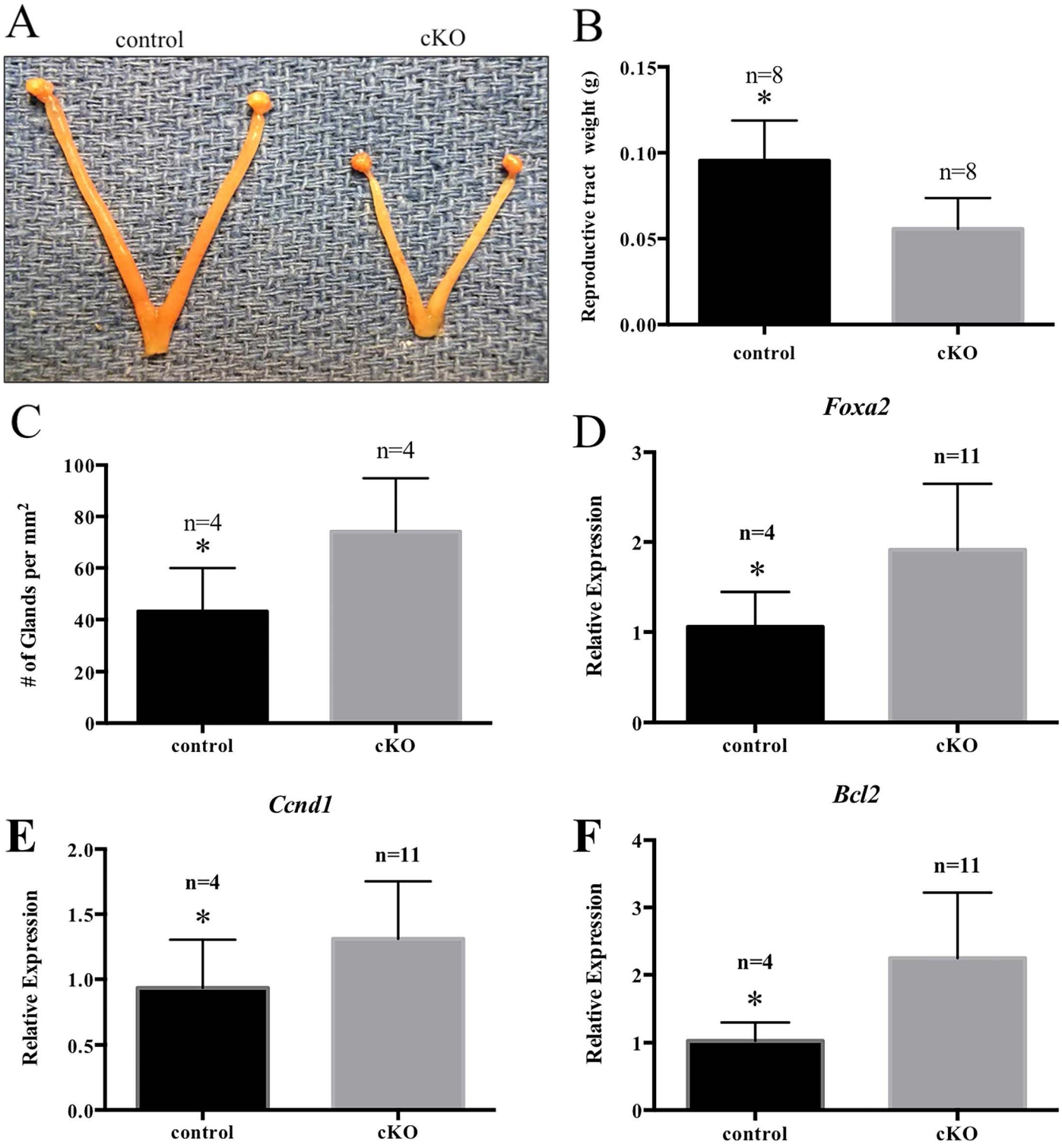


FIG. 3. Uteri from virgin *Arid1a* cKO mice were smaller. Uterine horns from 12-wk-old *Arid1a* cKO mice were shorter than those in control mice (**A**). Reproductive tracts from 12-wk-old cKO mice weighed less than those in control mice (**B**). Uteri from cKO mice displayed an increased number of uterine glands (**C**), consistent with increased levels of *Foxa2* expression as revealed by qPCR (**D**). Uteri from 12-wk-old cKO mice showed up-regulation of *Ccnd1* (**E**) and *Bcl2* (**F**). Statistical significance (*$P < 0.05$) was calculated by Student *t*-test. Relative Gene expression was relative to *Rpl13a*.

significant differences between virgin control and *Arid1a* cKO mice in FSH levels (control: 5.758 ± 0.625 ng/ml, n = 12; cKO: 7.270 ± 1.789 ng/ml, n = 10; Student *t*-test, $P = 0.402$) or LH levels (control: 0.406 ± 0.133 ng/ml, n = 12; cKO: 0.222 ± 0.0633 ng/ml, n = 10; Student *t*-test, $P = 0.253$). To evaluate steroid hormone production, we measured serum E2 levels in virgin adult unstimulated, randomly cycling mice. There were no significant differences in E2 levels between control (11.62 ± 7.437 pg/ml, n = 11) and *Arid1a* cKO (5.200 ± 1.078 pg/ml, n = 10; $P = 0.419$) mice.

In primigravid mice, at 4.5 dpc, P4 levels in *Arid1a* cKO pregnant mice (7.641 ± 2.296 ng/ml, n = 12) did not differ

TABLE 1. Number of implantation sites and resorbed embryos.

| Pregnancy number | Genotype | Embryonic day | Implantation sites/female (mean ± SD) | Viable embryos/female (mean ± SD) | % Resorbed embryos/female | *P*-value |
|---|---|---|---|---|---|---|
| 1 | Control | 8.5 (n = 8) | 9.1 ± 0.5 | 9.1 ± 0.5 | 0% | 0.9106 |
| | | 9.5 (n = 11) | 9.3 ± 0.4 | 9.3 ± 0.4 | 0% | 0.7749 |
| | | 16.5 (n = 11) | 8.1 ± 0.3 | 7.2 ± 0.4 | 10.3% | 0.7401 |
| 1 | cKO | 8.5 (n = 13) | 8.4 ± 0.3 | 8.2 ± 0.3 | 2.3% | |
| | | 9.5 (n = 8) | 8.4 ± 0.7 | 7.9 ± 0.8 | 8.3% | |
| | | 16.5 (n = 10) | 7.9 ± 0.4 | 6.5 ± 0.5 | 17.4% | |
| 3 | Control | 16.5 (n = 9)* | 11.2 ± 0.6 | 10.8 ± 0.6 | 4.1% | 0.0177* |
| | cKO | 16.5 (n = 8)* | 10.4 ± 0.5 | 8.3 ± 0.4 | 19.4% | |

* Statistical comparisons are between genotypes at similar embryonic day.

from those in control pregnant mice (14.57 ± 4.571 ng/ml, n = 11; $P = 0.426$), indicating normal luteal function. When *Arid1a* was deleted from the uterine epithelium using *Pgr-Cre*, there was a significant loss of *Pgr* expression as well as loss of expression of P4 responsive genes [21]. Therefore, we more closely examined steroid hormone receptor and steroid hormone response at the molecular level. Levels of *Pgr* (n > 4, $P = 0.194$) and estrogen receptor 1 (*Esr1*) (n > 4; Student *t*-test, $P = 0.817$) were similar between unstimulated virgin adult control and *Arid1a* cKO mice (Supplemental Fig. S6, A and B). To determine whether the uteri of *Arid1a* cKO mice show an altered response to steroid hormones, virgin unstimulated mice were ovariectomized and treated with E2 for 3 days or P4 for 6 h [67, 83]. The uteri from virgin *Arid1a* cKO females underwent a 5.2-fold increase in gross weight in response to E2, similar to the 5.8-fold increase observed for virgin control uteri (n = 6, Student *t*-test, $P = 0.3468$; Supplemental Fig. S6, C and D). Both control and *Arid1a* cKO uteri showed a significant increase in the estrogen responsive genes mucin 1 (*Muc1*), lactotransferrin (*Ltf*), and leukemia inhibitory factor *(Lif*) levels after E2 treatment (Supplemental Fig. S6, E–G). Furthermore, both virgin control and *Arid1a* cKO uteri showed a significant increase in expression of epithelial and stromal P4 responsive genes, Indian hedgehog (*Ihh*), cytochrome P450, family 26, subfamily A, polypeptide 1 (*Cyp26a1*), interleukin 13 receptor, alpha 2 (*Il13ra2*), heart and neural crest derivatives expressed transcript 2 (*Hand2*), and homeobox A10 (*Hoxa10*) levels in response to P4 (Supplemental Fig. S6, H–L). These results indicate that virgin *Arid1a* cKO uteri respond appropriately to E2 and P4.

### Arid1a *cKO Uteri Showed a Normal Decidualization Response*

To further investigate the subfertility phenotype, ovariectomized virgin control and *Arid1a* cKO mice were treated with hormones, and their uterus was mechanically stimulated to induce decidualization. Gross and histological morphology of the decidual and control horn were similar between virgin control and *Arid1a* cKO uteri (Supplemental Fig. S7, A–D). In addition, the ratio of decidualized to control horn weight was equivalent in control and *Arid1a* cKO uteri (n = 7; Student *t*-test, $P = 0.1748$; Supplemental Fig. S7E).

Primary cultures of human endometrial stromal fibroblasts (hESCs) have the ability to undergo in vitro decidualization, and this culture system has been used to demonstrate the importance of several factors in uterine decidualization, such as *LIF* [84], transient receptor potential cation channel, subfamily C, member 1 (*TRPC1*) [85], transcription factor 23 (*TCF23*) [86], uterine activing like kinase 2 (ALK2) [78], bone morphogenetic protein 2 (*BMP2*) [87], and *WNT4* [88]. Previous work has shown that ARID1A is deficient in hESCs from women with endometriosis [21] and that in vitro decidualization of hESCs from women with endometriosis have a blunted in vitro decidualization response [89]. To investigate the role of ARID1A in decidualization, we performed small interfering RNA knockdown of *ARID1A* in hESCs from women without endometriosis and then exposed cells to conditions for in vitro decidualization. HESCs transfected with siARID1A showed a 4.7-fold decrease in *ARID1A* compared with hESCs transfected with siNT (n = 7, Student *t*-test, $P < 0.001$; Supplemental Fig. S8A); hESCs transfected with siARID1A and then exposed to in vitro decidualization conditions showed changes in morphology similar to hESCs treated with siNT (data not shown). In addition, hESCs treated with siNT or siARID1A (n = 7) showed similar increases in levels of decidualization markers prolactin (*PRL*) (Student *t*-test, $P = 0.1441$), a ligand of the Wnt family (*WNT4*) (Student *t*-test, $P = 0.2146$), and insulin-like growth factor binding protein 1 (*IGFBP1*) (Student *t*-test, $P = 0.2591$; Supplemental Fig. S8, B–D). Therefore, knockdown of *ARID1A* in primary cultures of hESCs did not affect in vitro decidualization, similar to how deletion of *Arid1a* in stromal cells of the mouse uterus in vivo did not affect artificial decidualization (Supplemental Fig. S7).

### *Parous* Arid1a *cKO Mice Exhibited Reduced Fetal Viability*

Our fertility studies showed a progressive decline in the number of pups per litter, although female mice maintained normal decidualization. To investigate the time during pregnancy at which this phenotype becomes apparent, we performed timed pregnancy studies by breeding female control and *Arid1a* cKO mice at 6 wk with wild-type male mice. During the first pregnancy, for control mice, the number of implantation sites/female was similar to the number of viable embryos/female on Embryonic Days 8.5 and 9.5, with no resorbed embryos (Table 1 and Fig. 4A). By Embryonic Day 16.5, control mice had 10.3% resorbed embryos (Table 1). During the first pregnancy for *Arid1a* cKO mice, fewer implantation sites were observed on Embryonic Days 8.5 and 9.5 (Table 1 and Fig. 4B) compared to control. Additionally, *Arid1a* cKO females had 17.4% resorbed embryos on Embryonic Day 16.5 (Table 1). However, these differences between genotypes were not statistically significant (Table 1). Given the increase in resorbed embryos at Day 8.5, we examined the histology of implantation sites at this time point in the first pregnancy. We found hemorrhage and disruption in the implantation sites of primigravid *Arid1a* cKO uteri on Embryonic Day 8.5 (Fig. 4, C and D). Examination of the antimesometrial myometrium showed a significant thickening in primigravid *Arid1a* cKO mice compared with control mice

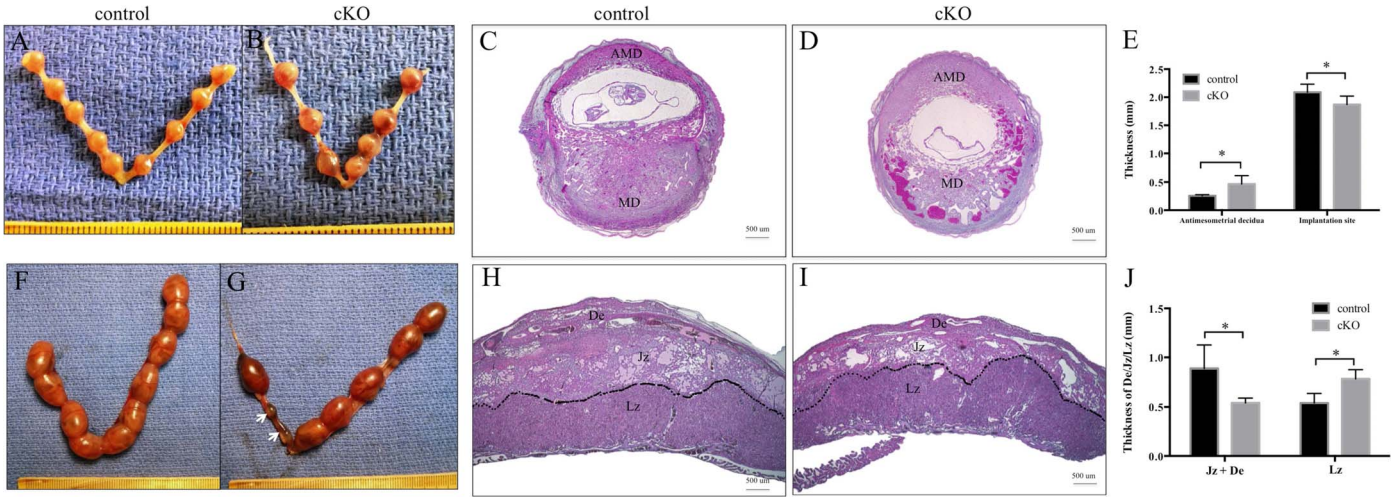


FIG. 4. *Arid1a* cKO mice showed increased embryo resorption during the third pregnancy. Gross morphology of primigravid control (**A**) and cKO (**B**) uteri on Embryonic Day 8.5. Conditional knockout implantation sites (**D**) on Embryonic Day 8.5 showed evidence of hemorrhage, which was not observed at control implantation sites (**C**). Conditional knockout antimesometrial decidua was thicker than those in control mice (**E**). Conditional knockout mice (**G**) showed more resorbed embryos (arrows) than control mice (**F**) on Embryonic Day 16.5 of the third pregnancy. Midsagittal sections of placental tissue obtained on Embryonic Day 16.5 from control (**H**) and cKO (**I**) mice of third pregnancy. Conditional knockout mice had a thinner junctional zone and decidua compared with control mice (**J**). AMD, antimesometrial decidua; MD, mesometrial decidua; De, decidua; Jz, junctional zone; Lz, labyrinthine zone; Statistical significance (*$P < 0.05$) was calculated by two-way ANOVA. Bars = 500 μm (**C**, **D**, **H**, **I**).

(Fig. 4E). Although the thickness of the implantation sites was less in primigravid *Arid1a* cKO mice than in control mice (Fig. 4E), there was no difference in the weight of viable implantation sites (data not shown).

Given the subfertility that began after the second pregnancy, we examined implantation sites in the third pregnancy. We discovered a statistically significant increase in the number of resorbed embryos in multigravida *Arid1a* cKO mice (19.4%) compared to multigravida control mice (4.1%, chi-square; $P = 0.0177$, Table 1 and Fig. 4, F and G). We performed histological examination of placentas from *Arid1a* cKO and control mice. On Embryonic Day 16.5 of the third pregnancy, placentas from *Arid1a* cKO mice exhibited thinner junctional and decidual zones than control mice (Fig. 4, H–J).

### *Molecular Differences Existed Between Parous and Virgin* Arid1a *cKO Mice*

To understand what factors contribute to the significant subfertility phenotype beginning with the third litter in *Arid1a* cKO mice, we studied multiparous females and their placentas. During the third pregnancy, P4 levels in multiparous *Arid1a* cKO pregnant mice at Embryonic Day 16.5 (23.34 ± 5.030 ng/ml, n = 7) did not differ from those in control pregnant mice (24.14 ± 5.886 ng/ml, n = 6; Student *t*-test, $P = 0.9195$), indicating normal luteal function in parous *Arid1a* cKO mice during pregnancy. Gross morphology and histology of parous ovaries was similar to virgin ovaries for both control and *Arid1a* cKO mice showing normal corpora lutea and follicular development (data not shown) further supporting normal luteal function in the first pregnancy and subsequent pregnancies. Finally, AMH levels were similar between virgin and multiparous *Arid1a* cKO mice (data not shown).

Recently, two different transforming growth factor beta-receptors, uterine activin like kinase 4 (ALK4) and uterine activin like kinase 5 (ALK5), were shown to significantly affect placental function when deleted in the uterus, leading to subfertility and sterility [90, 91]. Given the changes in placental morphology in parous *Arid1a* cKO females, we examined uterine differences at the molecular level for the underpinnings of this progressive subfertility phenotype. In uteri from 6-mo fertility studies, examination of ARID1A expression in the multiparous uterus showed a slight decrease in ARID1A expression. Expression of ARID1A was present in 50%–80% of epithelial cells in the uteri of *Arid1a* cKO female mice while expression of ARID1A was present in 80%–95% of epithelial cells in the uteri of control female mice (Fig. 5, A and B). Higher power magnification examination confirmed nuclear ARID1A staining in both *Arid1a* cKO uteri and control uteri with decreased expression in *Arid1a* cKO uteri (Supplemental Fig. S9). Previous work had shown that deletion of *Arid1a* with *Pgr-Cre* led to proliferation of uterine epithelial cells during early pregnancy, but not uterine stromal cells [21]. In parous uterus, we found that *Arid1a* cKO uterine epithelial and stromal cells showed increased proliferation compared to multiparous control (Fig. 5, C and D). However, there was no difference in PGR or ESR1 expression (Fig. 5, E–H). These data suggest that ARID1A plays a role in both epithelial and stromal cell proliferation in the uterus. Given the subtle changes in thickness of antimesometrium at Embryonic Day 8.5 in the first pregnancy and the more significant changes in placental morphology at Embryonic Day 16.5 in the third pregnancy, we focused our molecular studies on the placenta.

We discovered a 33% decrease in *Arid1a* expression in the placentas from *Arid1a* cKO mothers during the third pregnancy (Fig. 6A), likely an indirect effect and not an effect of knockout on the placenta. Similarly, there was a significant decrease in SWI/SNF related, matrix associated, actin dependent regulator of chromatin, subfamily A, member 4 (*Smarca4*), an ARID1A binding partner, expression (Fig. 6B). To gain insight into the molecular underpinnings of the placental phenotype, we examined the levels of molecules involved in placental structure and function. We discovered decreased expression of nodal growth differentiation factor (*Nodal*), a transforming growth factor beta-receptor ligand (Fig. 6C) in placentas from *Arid1a* cKO female mice. Additionally, placentas from *Arid1a* cKO mice exhibited decreased protocadherin 12 (*Pcdh12*), a marker of glycogen trophoblast cells, and trophoblast specific protein alpha (*Tphpa*), a marker of spongiotrophoblast cells compared to placentas from control female mice (Fig. 6, D and

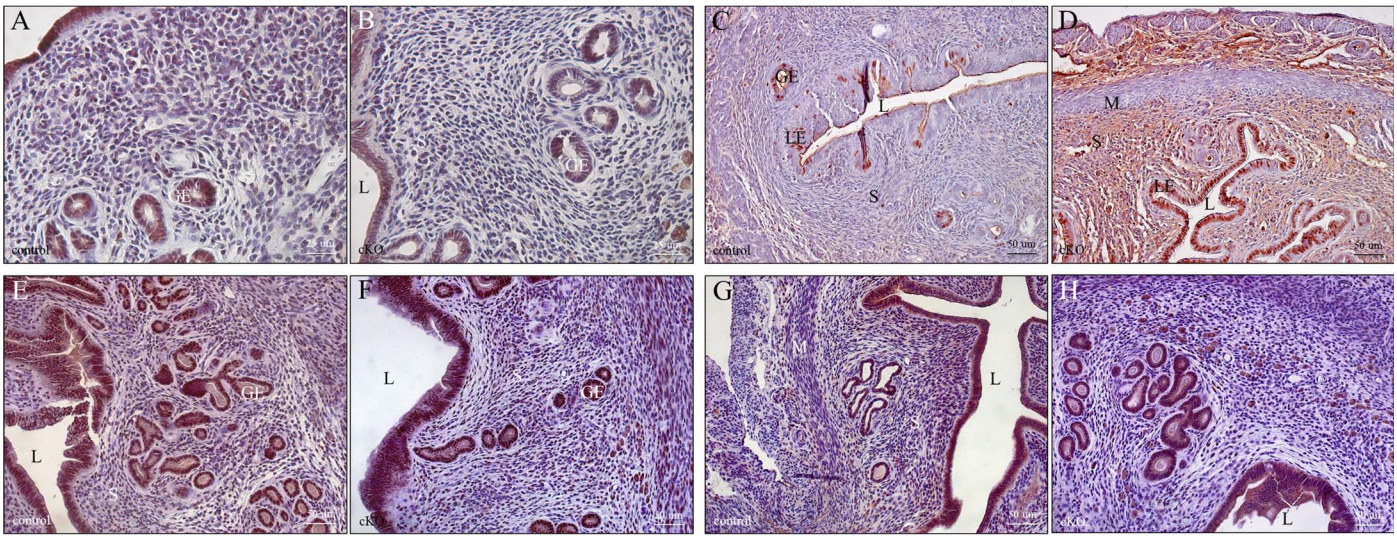


FIG. 5. After 6-mo fertility studies, parous uteri from *Arid1a* cKO mice showed increased proliferation. ARID1A expression was present in >95% of epithelial cells from control (**A**) but only 50%–80% of epithelial cells from cKO (**B**) uteri. However, increased proliferation in both epithelium and stromal compartments was apparent in cKO (**D**) compared to control (**C**) parous uteri by Ki67 staining. Expression of ESR1was similar between control (**E**) and cKO (**F**) parous uteri. Similarly, expression of PGR was similar between control (**G**) and cKO parous uteri (**H**). GE, glandular epithelium; L, lumen; LE, luminal epithelium; M, myometrium; S, uterine stroma. Bars = 25 μm (**A**, **B**) and 50 μm (**C**–**H**).

E). Compared with placentas from control female mice, placentas from *Arid1a* cKO female mice showed significantly lower levels of *Ptgs2* (Fig. 6F), which is important for ectoplacental cone formation [92]. Levels of molecules involved in vasculogenesis (*Vegfa*) and angiogenesis (*Angpt1*) were also significantly decreased in placentas from cKO females (Fig. 6, G and H). Furthermore, levels of *Corin,* which is critical for trophoblast invasion [93], were significantly reduced in placentas from *Arid1a* cKO females (Fig. 6I). There were no differences between genotypes in levels of *Gcm1,* which is important for chorioallontoic branching [94], or *Vcam1,* which is critical for vascular endothelium formation [95] (Fig. 6, J and K).

## DISCUSSION

Many previous studies have focused on the role of ARID1A in cancer, particularly as a tumor suppressor or driver mutation in tumors of the female reproductive tract [9, 11, 13, 15, 20, 23]. Thus, our original hypothesis was that deletion of *Arid1a* with *Amhr2-Cre* would give rise to ovarian tumors in mice. Here, by conditionally deleting *Arid1a* in mesenchymal-derived cells of the female reproductive tract, we provide evidence that loss of *Arid1a* is not sufficient for tumor formation, suggesting that additional mutations are required for tumor formation in the mouse female reproductive tract. However, we show that ARID1A is important for normal placental morphology and fertility in parous female mice. Female mice with conditional deletion of *Arid1a* show a progressive decline in fertility with higher parity, with a loss of pups in the postimplantation phase beginning with the third pregnancy.

Studies suggest that ARID1A plays a key role in the proliferation of several types of cancers and is associated with genetic aberrations in cyclin-dependent kinases [96]. For colon cancer, non-small cell lung cancer, and gastric cancer, knockdown of *ARID1A* enhances cellular proliferation in vitro, and restoration of *ARID1A* expression suppresses cellular proliferation [82, 97, 98]. Likewise, we found that loss of *Arid1a* up-regulated *Ccnd1* in the virgin uterus in vivo. Additionally, we also observed up-regulation of the pro-apoptotic gene *Bcl2* in the *Arid1a* cKO uterus. Therefore, we believe that the balance of proliferation and apoptosis may preclude the development of cancer in virgin female *Arid1a* cKO mice. Other studies using adenovirus-driven *Cre* to delete *Arid1a* from the ovarian surface epithelium showed that *Arid1a* depletion is not sufficient to induce ovarian tumors in mice [22]. Additionally, our work deleting *Arid1a* in the uterus using *Pgr-Cre* did not develop endometrial tumors [21]. Consistently, we found that *Arid1a* deletion from the ovarian surface epithelium using *Amhr2-Cre* did not induce ovarian tumors in virgin female mice. Thus, we speculate that female reproductive tract cancers in mice require additional genetic hits along with loss of *Arid1a* to give rise to malignant tumors.

Interestingly, *Arid1a* cKO female mice had significant subfertility that became apparent after the second pregnancy. Translationally, this may be comparable to secondary infertility although most of our *Arid1a* cKO mice were not completely infertile. Male factors did not contribute because we were using fertility-proven intact wild-type male mice for our experiments. Given the deletion of *Arid1a* in the somatic cells of the ovary, ovarian dysfunction was critically evaluated. In primigravid and multigravida female *Arid1a* cKO mice, we found similar P4 levels as control as well as similar numbers of corpora lutea. AMH levels, a measure of ovarian reserve, were also similar between *Arid1a* cKO and control for both virgin and parous female mice. Gonadotropin levels were also similar between virgin *Arid1a* cKO and control female mice. Thus, we do not see an obvious luteal phase defect or other ovulatory dysfunction in either virgin or parous *Arid1a* cKO female mice. However, it remains possible that a more subtle luteal defect may contribute to the reduced pups per litter. Anatomically, *Arid1a* cKO had normal oviductal, uterine, and cervical histology for both virgin and parous female mice, and we found no gross or histological evidence of endometriosis. Thus, we do not believe that anatomical factors lead to secondary subfertility. In women undergoing an evaluation for secondary infertility, this would fall under the category of unexplained infertility and is typically thought to be caused by endometrial dysfunction. Only recently have genomewide

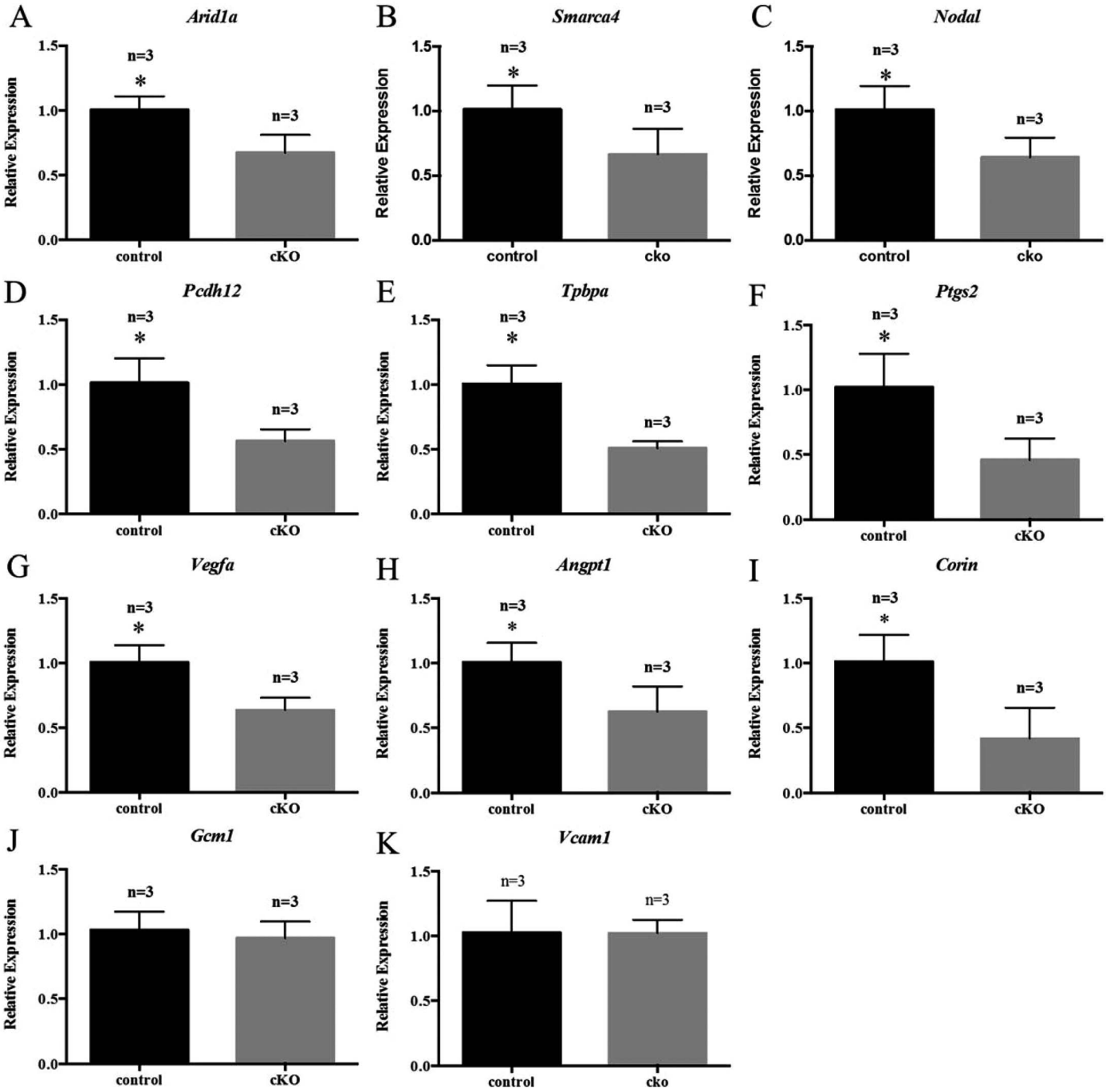


FIG. 6. Placentas from *Arid1a* cKO mice showed molecular dysregulation. Placental mRNA levels of *Arid1a* (**A**), *Smarca4* (**B**), *Nodal* (**C**), *Pcdh12* (**D**), *Tpbpa* (**E**), *Ptgs2* (**F**), *Vegfa* (**G**), *Angpt1* (**H**), and *Corin* (**I**) were decreased in cKO mice on Embryonic Day 16.5 of the third pregnancy. There was no difference in levels of *Gcm1* (**J**) or *Vcam1* (**K**). Statistical significance (*$P < 0.05$) was calculated by Student *t*-test. Gene expression was measured relative to *Gapdh*.

profiling techniques been used to identify these subtle molecular changes [99–101].

Our virgin *Arid1a* cKO female mice had normal implantation, normal decidualization, and normal pregnancy outcomes in the first pregnancy. However, examination of parous uteri showed an increase in both epithelial and stromal proliferation (Fig. 5) with deletion of ARID1A that was not present in virgin uteri even at 1 yr of age (data not shown). Little has been published about the molecular differences between virgin and parous uteri. We can only speculate that the deletion of *Arid1a* led to indirect changes in gene expression that affected uterine remodeling after pregnancy. We speculate that subtle changes in the uterine stroma after remodeling postpartum lead to changes in placentation with subsequent pregnancies. However, significant work needs to be done to understand the subtle molecular changes between the parous and the virgin uterus before we can tease out the specific changes associated with loss of *Arid1a*.

Only after pregnancy, one female *Arid1a* cKO mouse was found to have a benign uterine tumor that exhibited a lack of ARID1A in epithelial cells. Given the low penetrance (one in nine) of tumors in parous uteri, a significantly larger number of

female mice would need to be examined to determine the statistical significance of this result. Previous studies suggest that glandular and luminal epithelial cells of the uterus are regenerated from uterine stromal cells after pregnancy in *Amhr2-Cre* mice [102]. After one pregnancy, at most 50% of epithelial cells were regenerated from stroma in a process of mesenchymal epithelial transition (MET) [103]. Thus, depletion of ARID1A in the epithelium could result from *Arid1a* deletion in uterine stromal cells. This could account for the loss of ARID1A in the one female mouse with a tumor after pregnancy. Interestingly, recurrent copy number variants of *Arid1a* have recently been discovered in uterine leiomyomata tumors [104], which are the most translationally equivalent human disease to the one tumor. However, other parous *Arid1a* cKO female mice examined had expression of ARID1A in the epithelium and no tumors. Deletion of *Arid1a* with *Pgr-Cre* deleted *Arid1a* in the epithelium and did not result is similar tumors. However, these female mice were completely sterile and thus could not be studied in the multiparous state [21].

Indeed, we did see a decrease in ARID1A staining in the epithelium after repetitive pregnancy (Fig. 5 and Supplemental Fig. 9) in *Arid1a* cKO uteri, suggesting that MET is occurring in this model. Similar to published work, we saw at most 50% loss of ARID1A staining in epithelial cells after repetitive pregnancy. While previous work had only examined MET after 1 pregnancy, we have shown that MET remains after repetitive pregnancies and may be long lasting. The MET effect does not seem to be exponential with each pregnancy (i.e., loss of 50% with first pregnancy, loss of another 50% with second pregnancy). However, we cannot speculate as to whether repetitive pregnancy allows for regeneration of ARID1A-positive epithelial cells from ARID1A-positive epithelial cells based on our experimental time point. While a partial deletion of ARID1A does occur in the epithelial cells of the uterus in the *Arid1a* cKO mice, the phenotype is different than the complete deletion of ARID1A in the epithelial cells of the uterus of the *Pgr-Cre* female mice. However, it remains possible that the epithelial cell phenotype in the Amhr2-Cre female mice contributes to the reduced pups per litter.

Finally, multiparous *Arid1a* cKO female mice developed significantly abnormal placentas. The placenta is critical for proper fetal development. Translationally, placental abnormalities can lead to significant maternal morbidities such as preeclampsia and fetal complications such as fetal growth restriction or fetal demise. While we did not find gross differences in size of live born pups (data not shown), we did discover significant resorption of embryos at Embryonic Day 16.5 in the third litter of *Arid1a* cKO female mice (Table 1and Fig. 4). The placental morphology was abnormal (Fig. 4), and molecular markers of abnormal placental morphology confirmed these differences (Fig. 6). ARID1A is a critical player in chromatin remodeling, cellular proliferation, and gene regulation [2, 104–108]. Although multiple studies have focused on the role of epigenetic markers in chromatin remodeling in the placenta, little is known about the actual gene products involved in placental chromatin remodeling. One study shows that in vitro depletion of *SMARCA4* (also known as BRG1), which is a critical member of the SWI/SNF chromatin-remodeling complex and a known protein-binding partner for ARID1A [109] that plays a key role in trophoblast stem cell self-renewal [110], has a similar effect on cellular proliferation as the depletion of ARID1A [111]. We found a decrease in both *Arid1a* and *Smarca4* expression in placentas from multiparous *Arid1a* cKO females (Fig. 6). In the present study, the molecular markers examined in placentas from *Arid1a* cKO mice are at best suggestive of abnormal placental morphology. Although they do not provide a complete understanding of the molecular mechanism of the effect of *Arid1a* deletion, they suggest that loss of *Arid1a* in the uterus impairs placental function, evidenced by a subfertility phenotype, increased resorbed embryos, and a thinner junctional zone at implantation sites.

In conclusion, we found that *Arid1a* deletion alone is insufficient to induce tumorigenesis in the female reproductive tract of mice. ARID1A regulates embryo implantation and development of a functional placenta. Future studies of our *Arid1a* cKO mouse model should provide molecular insight into the delicate function of SWI/SNF-mediated chromatin remodeling in placental function.

## ACKNOWLEDGMENT

We thank Monica Logan, A. Theresa Wittman, and Mahitha Ravi for their technical support.

## REFERENCES

1. Hargreaves DC, Crabtree GR. ATP-dependent chromatin remodeling: genetics, genomics and mechanisms. Cell Res 2011; 21:396–420.
2. Nagl NG Jr, Patsialou A, Haines DS, Dallas PB, Beck GR Jr, Moran E. The p270 (ARID1A/SMARCF1) subunit of mammalian SWI/SNF-related complexes is essential for normal cell cycle arrest. Cancer Res 2005; 65:9236–9244.
3. Jones S, Li M, Parsons DW, Zhang X, Wesseling J, Kristel P, Schmidt MK, Markowitz S, Yan H, Bigner D, Hruban RH, Eshleman JR, Iacobuzio-Donahue CA, et al. Somatic mutations in the chromatin remodeling gene ARID1A occur in several tumor types. Hum Mutat 2012; 33:100–103.
4. Park JH, Lee C, Suh JH, Chae JY, Kim HW, Moon KC. Decreased ARID1A expression correlates with poor prognosis of clear cell renal cell carcinoma. Hum Pathol 2015; 46:454–460.
5. Wang K, Kan J, Yuen ST, Shi ST, Chu KM, Law S, Chan TL, Kan Z, Chan AS, Tsui WY, Lee SP, Ho SL, et al. Exome sequencing identifies frequent mutation of ARID1A in molecular subtypes of gastric cancer. Nat Genet 2011; 43:1219–1223.
6. Balbas-Martinez C, Rodriguez-Pinilla M, Casanova A, Dominguez O, Pisano DG, Gomez G, Lloreta J, Lorente JA, Malats N, Real FX. ARID1A alterations are associated with FGFR3-wild type, poor-prognosis, urothelial bladder tumors. PLoS One 2013; 8:e62483.
7. Mamo A, Cavallone L, Tuzmen S, Chabot C, Ferrario C, Hassan S, Edgren H, Kallioniemi O, Aleynikova O, Przybytkowski E, Malcolm K, Mousses S, et al. An integrated genomic approach identifies ARID1A as a candidate tumor-suppressor gene in breast cancer. Oncogene 2012; 31: 2090–2100.
8. Wiegand KC, Shah SP, Al-Agha OM, Zhao Y, Tse K, Zeng T, Senz J, McConechy MK, Anglesio MS, Kalloger SE, Yang W, Heravi-Moussavi A, et al. ARID1A mutations in endometriosis-associated ovarian carcinomas. N Engl J Med 2010; 363:1532–1543.
9. Wiegand KC, Lee AF, Al-Agha OM, Chow C, Kalloger SE, Scott DW, Steidl C, Wiseman SM, Gascoyne RD, Gilks B, Huntsman DG. Loss of BAF250a (ARID1A) is frequent in high-grade endometrial carcinomas. J Pathol 2011; 224:328–333.
10. Wiegand KC, Hennessy BT, Leung S, Wang Y, Ju Z, McGahren M, Kalloger SE, Finlayson S, Stemke-Hale K, Lu Y, Zhang F, Anglesio MS, et al. A functional proteogenomic analysis of endometrioid and clear cell carcinomas using reverse phase protein array and mutation analysis: protein expression is histotype-specific and loss of ARID1A/BAF250a is associated with AKT phosphorylation. BMC Cancer 2014; 14:120.
11. Jones S, Wang TL, Ie-Ming S, Mao T-L, Nakayama K, Roden R, Glas R, Slamon D, Diaz LA Jr, Vogelstein B, Kinzler KW, Velculescu VE, Papadopoulos N. Frequent mutations of chromatin remodeling gene ARID1A in ovarian clear cell carcinoma. Science 2010; 330:228–231.
12. Birnbaum DJ, Adelaide J, Mamessier E, Finetti P, Lagarde A, Monges G, Viret F, Goncalves A, Turrini O, Delpero JR, Iovanna J, Giovannini M, et al. Genome profiling of pancreatic adenocarcinoma. Genes Chromosomes Cancer 2011; 50:456–465.
13. Guan B, Mao TL, Panuganti PK, Kuhn E, Kurman RJ, Maeda D, Chen E, Jeng YM, Wang TL, Ie-Ming S. Mutation and loss of expression of ARID1A in uterine low-grade endometrioid carcinoma. Am J Surg Pathol 2011; 35:625–632.

14. Huang J, Zhao YL, Li Y, Fletcher JA, Xiao S. Genomic and functional evidence for an ARID1A tumor suppressor role. Genes Chromosomes Cancer 2007; 46:745–750.
15. Liang H, Cheung LW, Li J, Ju Z, Yu S, Stemke-Hale K, Dogruluk T, Lu Y, Liu X, Gu C, Guo W, Scherer SE, et al. Whole-exome sequencing combined with functional genomics reveals novel candidate driver cancer genes in endometrial cancer. Genome Res 2012; 22:2120–2129.
16. Luo B, Cheung HW, Subramanian A, Sharifnia T, Okamoto M, Yang X, Hinkle G, Boehm JS, Beroukhim R, Weir BA, Mermel C, Barbie DA, et al. Highly parallel identification of essential genes in cancer cells. Proc Natl Acad Sci U S A 2008; 105:20380–20385.
17. Pottier N, Yang W, Assem M, Panetta JC, Pei D, Paugh SW, Cheng C, Den Boer ML, Relling MV, Pieters R, Evans WE, Cheok MH. The SWI/SNF chromatin-remodeling complex and glucocorticoid resistance in acute lymphoblastic leukemia. J Natl Cancer Inst 2008; 100:1792–1803.
18. Wang X, Nagl NG Jr, Flowers S, Zweitzig D, Dallas PB, Moran E. Expression of p270 (ARID1A), a component of human SWI/SNF complexes, in human tumors. Int J Cancer 2004; 112:636.
19. Cancer Genome Atlas Research Network, Kandoth C, Schultz N, Cherniack AD, Akbani R, Liu Y, Shen H, Robertson AG, Pashtan I, Shen R, Benz CC, Yau C, et al. Integrated genomic characterization of endometrial carcinoma. Nature 2013; 497:67–73.
20. Guan B, Wang TL, Ie-Ming S. ARID1A, a factor that promotes formation of SWI/SNF-mediated chromatin remodeling, is a tumor suppressor in gynecologic cancers. Cancer Res 2011; 71:6718–6727.
21. Kim TH, Yoo JY, Wang Z, Lydon JP, Khatri S, Hawkins SM, Leach RE, Fazleabas AT, Young SL, Lessey BA, Ku BJ, Jeong JW. ARID1A is essential for endometrial function during early pregnancy. PLoS Genet 2015; 11:e1005537.
22. Guan B, Rahmanto YS, Wu RC, Wang Y, Wang Z, Wang TL, Ie-Ming S. Roles of deletion of Arid1a, a tumor suppressor, in mouse ovarian tumorigenesis. J Natl Cancer Inst 2014; 106.
23. Chandler RL, Damrauer JS, Raab JR, Schisler JC, Wilkerson MD, Didion JP, Starmer J, Serber D, Yee D, Xiong J, Darr DB, Pardo-Manuel de Villena F, et al. Coexistent ARID1A-PIK3CA mutations promote ovarian clear-cell tumorigenesis through pro-tumorigenic inflammatory cytokine signalling. Nat Commun 2015; 6:6118.
24. Gao X, Tate P, Hu P, Tjian R, Skarnes WC, Wang Z. ES cell pluripotency and germ-layer formation require the SWI/SNF chromatin remodeling component BAF250a. Proc Natl Acad Sci U S A 2008; 105: 6656–6661.
25. Lei I, Gao X, Sham MH, Wang Z. SWI/SNF protein component BAF250a regulates cardiac progenitor cell differentiation by modulating chromatin accessibility during second heart field development. J Biol Chem 2012; 287:24255–24262.
26. Jamin SP, Arango NA, Mishina Y, Hanks MC, Behringer RR. Requirement of Bmpr1a for Mullerian duct regression during male sexual development. Nat Genet 2002; 32:408–410.
27. Jamin SP, Arango NA, Mishina Y, Hanks MC, Behringer RR. Genetic studies of the AMH/MIS signaling pathway for Mullerian duct regression. Mol Cell Endocrinol 2003; 211:15–19.
28. Mullany LK, Fan HY, Liu Z, White LD, Marshall A, Gunaratne P, Anderson ML, Creighton CJ, Xin L, Deavers M, Wong KK, Richards JS. Molecular and functional characteristics of ovarian surface epithelial cells transformed by KrasG12D and loss of Pten in a mouse model in vivo. Oncogene 2011; 30:3522–3536.
29. Deutscher E, Hung-Chang Yao H. Essential roles of mesenchyme-derived beta-catenin in mouse Mullerian duct morphogenesis. Dev Biol 2007; 307:227–236.
30. Arango NA, Kobayashi A, Wang Y, Jamin SP, Lee HH, Orvis GD, Behringer RR. A mesenchymal perspective of Mullerian duct differentiation and regression in Amhr2-lacZ mice. Mol Reprod Dev 2008; 75: 1154–1162.
31. Zeng F, Baldwin DA, Schultz RM. Transcript profiling during preimplantation mouse development. Dev Biol 2004; 272:483–496.
32. Sargent KM, Lu N, Clopton DT, Pohlmeier WE, Brauer VM, Ferrara N, Silversides DW, Cupp AS. Loss of vascular endothelial growth factor A (VEGFA) isoforms in granulosa cells using pDmrt-1-Cre or Amhr2-Cre reduces fertility by arresting follicular development and by reducing litter size in female mice. PLoS One 2015; 10:e0116332.
33. Yu Z, Kim J, He L, Creighton CJ, Gunaratne PH, Hawkins SM, Matzuk MM. Functional analysis of miR-34c as a putative tumor suppressor in high-grade serous ovarian cancer. Biol Reprod 2014; 91:113.
34. Robker RL, Watson LN, Robertson SA, Dunning KR, McLaughlin EA, Russell DL. Identification of sites of STAT3 action in the female reproductive tract through conditional gene deletion. PLoS One 2014; 9: e101182.
35. Gao Y, Li S, Li Q. Uterine epithelial cell proliferation and endometrial hyperplasia: evidence from a mouse model. Mol Hum Reprod 2014; 20: 776–786.
36. Mullany LK, Liu Z, King ER, Wong KK, Richards JS. Wild-type tumor repressor protein 53 (Trp53) promotes ovarian cancer cell survival. Endocrinology 2012; 153:1638–1648.
37. Fan HY, Liu Z, Paquet M, Wang J, Lydon JP, DeMayo FJ, Richards JS. Cell type-specific targeted mutations of Kras and Pten document proliferation arrest in granulosa cells versus oncogenic insult to ovarian surface epithelial cells. Cancer Res 2009; 69:6463–6472.
38. Xing D, Scangas G, Nitta M, He L, Xu X, Ioffe YJ, Aspuria PJ, Hedvat CY, Anderson ML, Oliva E, Karlan BY, Mohapatra G, et al. A role for BRCA1 in uterine leiomyosarcoma. Cancer Res 2009; 69:8231–8235.
39. Lague MN, Paquet M, Fan HY, Kaartinen MJ, Chu S, Jamin SP, Behringer RR, Fuller PJ, Mitchell A, Dore M, Huneault LM, Richards JS, et al. Synergistic effects of Pten loss and WNT/CTNNB1 signaling pathway activation in ovarian granulosa cell tumor development and progression. Carcinogenesis 2008; 29:2062–2072.
40. Daikoku T, Jackson L, Besnard V, Whitsett J, Ellenson LH, Dey SK. Cell-specific conditional deletion of Pten in the uterus results in differential phenotypes. Gynecol Oncol 2011; 122:424–429.
41. Lague MN, Detmar J, Paquet M, Boyer A, Richards JS, Adamson SL, Boerboom D. Decidual PTEN expression is required for trophoblast invasion in the mouse. Am J Physiol Endocrinol Metab 2010; 299: E936–E946.
42. Kim J, Coffey DM, Creighton CJ, Yu Z, Hawkins SM, Matzuk MM. High-grade serous ovarian cancer arises from fallopian tube in a mouse model. Proc Natl Acad Sci U S A 2012; 109:3921–3926.
43. Mullany LK, Liu Z, Wong KK, Deneke V, Ren YA, Herron A, Richards JS. Tumor repressor protein 53 and steroid hormones provide a new paradigm for ovarian cancer metastases. Mol Endocrinol 2014; 28: 127–137.
44. Stewart CA, Wang Y, Bonilla-Claudio M, Martin JF, Gonzalez G, Taketo MM, Behringer RR. CTNNB1 in mesenchyme regulates epithelial cell differentiation during Mullerian duct and postnatal uterine development. Mol Endocrinol 2013; 27:1442–1454.
45. Zhang L, Patterson AL, Zhang L, Teixeira JM, Pru JK. Endometrial stromal beta-catenin is required for steroid-dependent mesenchymal-epithelial cross talk and decidualization. Reprod Biol Endocrinol 2012; 10:75.
46. Boerboom D, Paquet M, Hsieh M, Liu J, Jamin SP, Behringer RR, Sirois J, Taketo MM, Richards JS. Misregulated Wnt/beta-catenin signaling leads to ovarian granulosa cell tumor development. Cancer Res 2005; 65: 9206–9215.
47. Boerboom D, White LD, Dalle S, Courty J, Richards JS. Dominant-stable beta-catenin expression causes cell fate alterations and Wnt signaling antagonist expression in a murine granulosa cell tumor model. Cancer Res 2006; 66:1964–1973.
48. Daikoku T, Yoshie M, Xie H, Sun X, Cha J, Ellenson LH, Dey SK. Conditional deletion of Tsc1 in the female reproductive tract impedes normal oviductal and uterine function by enhancing mTORC1 signaling in mice. Mol Hum Reprod 2013; 19:463–472.
49. Tanaka Y, Park JH, Tanwar PS, Kaneko-Tarui T, Mittal S, Lee HJ, Teixeira JM. Deletion of tuberous sclerosis 1 in somatic cells of the murine reproductive tract causes female infertility. Endocrinology 2012; 153:404–416.
50. Migone FF, Ren Y, Cowan RG, Harman RM, Nikitin AY, Quirk SM. Dominant activation of the hedgehog signaling pathway alters development of the female reproductive tract. Genesis 2012; 50:28–40.
51. Ren Y, Cowan RG, Migone FF, Quirk SM. Overactivation of hedgehog signaling alters development of the ovarian vasculature in mice. Biol Reprod 2012; 86:174.
52. Harman RM, Cowan RG, Ren Y, Quirk SM. Reduced signaling through the hedgehog pathway in the uterine stroma causes deferred implantation and embryonic loss. Reproduction 2011; 141:665–674.
53. Ren Y, Cowan RG, Harman RM, Quirk SM. Dominant activation of the hedgehog signaling pathway in the ovary alters theca development and prevents ovulation. Mol Endocrinol 2009; 23:711–723.
54. Wang Y, Jia Y, Franken P, Smits R, Ewing PC, Lydon JP, DeMayo FJ, Burger CW, Anton Grootegoed J, Fodde R, Blok LJ. Loss of APC function in mesenchymal cells surrounding the Mullerian duct leads to myometrial defects in adult mice. Mol Cell Endocrinol 2011; 341:48–54.
55. Boyer A, Goff AK, Boerboom D. WNT signaling in ovarian follicle biology and tumorigenesis. Trends Endocrinol Metab 2010; 21:25–32.
56. Lei L, Jin S, Gonzalez G, Behringer RR, Woodruff TK. The regulatory role of Dicer in folliculogenesis in mice. Mol Cell Endocrinol 2010; 315: 63–73.

57. Gonzalez G, Behringer RR. Dicer is required for female reproductive tract development and fertility in the mouse. Mol Reprod Dev 2009; 76: 678–688.
58. Nagaraja AK, Andreu-Vieyra C, Franco HL, Ma L, Chen R, Han DY, Zhu H, Agno JE, Gunaratne PH, DeMayo FJ, Matzuk MM. Deletion of Dicer in somatic cells of the female reproductive tract causes sterility. Mol Endocrinol 2008; 22:2336–2352.
59. Petit FG, Jamin SP, Kurihara I, Behringer RR, DeMayo FJ, Tsai MJ, Tsai SY. Deletion of the orphan nuclear receptor COUP-TFII in uterus leads to placental deficiency. Proc Natl Acad Sci U S A 2007; 104:6293–6298.
60. Jeyasuria P, Ikeda Y, Jamin SP, Zhao L, De Rooij DG, Themmen AP, Behringer RR, Parker KL. Cell-specific knockout of steroidogenic factor 1 reveals its essential roles in gonadal function. Mol Endocrinol 2004; 18:1610–1619.
61. Pangas SA, Jorgez CJ, Tran M, Agno J, Li X, Brown CW, Kumar TR, Matzuk MM. Intraovarian activins are required for female fertility. Mol Endocrinol 2007; 21:2458–2471.
62. Jorgez CJ, Klysik M, Jamin SP, Behringer RR, Matzuk MM. Granulosa cell-specific inactivation of follistatin causes female fertility defects. Mol Endocrinol 2004; 18:953–967.
63. Pangas SA, Li X, Umans L, Zwijsen A, Huylebroeck D, Gutierrez C, Wang D, Martin JF, Jamin SP, Behringer RR, Robertson EJ, Matzuk MM. Conditional deletion of Smad1 and Smad5 in somatic cells of male and female gonads leads to metastatic tumor development in mice. Mol Cell Biol 2008; 28:248–257.
64. Pangas SA, Li X, Robertson EJ, Matzuk MM. Premature luteinization and cumulus cell defects in ovarian-specific Smad4 knockout mice. Mol Endocrinol 2006; 20:1406–1422.
65. Gigli I, Cushman RA, Wahl CM, Fortune JE. Evidence for a role for anti-Mullerian hormone in the suppression of follicle activation in mouse ovaries and bovine ovarian cortex grafted beneath the chick chorioallantoic membrane. Mol Reprod Dev 2005; 71:480–488.
66. Hawkins SM, Andreu-Vieyra CV, Kim TH, Jeong JW, Hodgson MC, Chen R, Creighton CJ, Lydon JP, Gunaratne PH, DeMayo FJ, Matzuk MM. Dysregulation of uterine signaling pathways in progesterone receptor-Cre knockout of dicer. Mol Endocrinol 2012; 26:1552–1566.
67. Jeong JW, Lee KY, Kwak I, White LD, Hilsenbeck SG, Lydon JP, DeMayo FJ. Identification of murine uterine genes regulated in a ligand-dependent manner by the progesterone receptor. Endocrinology 2005; 146:3490–3505.
68. Large MJ, Wetendorf M, Lanz RB, Hartig SM, Creighton CJ, Mancini MA, Kovanci E, Lee KF, Threadgill DW, Lydon JP, Jeong JW, DeMayo FJ. The epidermal growth factor receptor critically regulates endometrial function during early pregnancy. PLoS Genet 2014; 10:e1004451.
69. Finn CA, Martin L. Endocrine control of the timing of endometrial sensitivity to a decidual stimulus. Biol Reprod 1972; 7:82–86.
70. Varani S, Elvin JA, Yan C, DeMayo J, DeMayo FJ, Horton HF, Byrne MC, Matzuk MM. Knockout of pentraxin 3, a downstream target of growth differentiation factor-9, causes female subfertility. Mol Endocrinol 2002; 16:1154–1167.
71. Schroder AL, Pelch KE, Nagel SC. Estrogen modulates expression of putative housekeeping genes in the mouse uterus. Endocrine 2009; 35: 211–219.
72. Sato TA, Gupta DK, Keelan JA, Marvin KW, Mitchell MD. Cytosolic phospholipase A(2)and 15-hydroxyprostaglandin dehydrogenase mRNA expression in murine uterine and gestational tissues during late pregnancy. Prostaglandins Leukot Essent Fatty Acids 2001; 64:247–251.
73. Rampon C, Bouillot S, Climescu-Haulica A, Prandini MH, Cand F, Vandenbrouck Y, Huber P. Protocadherin 12 deficiency alters morphogenesis and transcriptional profile of the placenta. Physiol Genomics 2008; 34:193–204.
74. Ayakannu T, Taylor AH, Willets JM, Brown L, Lambert DG, McDonald J, Davies Q, Moss EL, Konje JC. Validation of endogenous control reference genes for normalizing gene expression studies in endometrial carcinoma. Mol Hum Reprod 2015; 21:723–735.
75. Aghajanova L, Tatsumi K, Horcajadas JA, Zamah AM, Esteban FJ, Herndon CN, Conti M, Giudice LC. Unique transcriptome, pathways, and networks in the human endometrial fibroblast response to progesterone in endometriosis. Biol Reprod 2011; 84:801–815.
76. Hawkins SM, Creighton CJ, Han DY, Zariff A, Anderson ML, Gunaratne PH, Matzuk MM. Functional microRNA involved in endometriosis. Mol Endocrinol 2011; 25:821–832.
77. Livak KJ, Schmittgen TD. Analysis of relative gene expression data using real-time quantitative PCR and the 2(-Delta Delta C(T)) Method. Methods 2001; 25:402–408.
78. Clementi C, Tripurani SK, Large MJ, Edson MA, Creighton CJ, Hawkins SM, Kovanci E, Kaartinen V, Lydon JP, Pangas SA, DeMayo FJ, Matzuk MM. Activin-like kinase 2 functions in peri-implantation uterine signaling in mice and humans. PLoS Genet 2013; 9:e1003863.
79. Besnard V, Wert SE, Hull WM, Whitsett JA. Immunohistochemical localization of Foxa1 and Foxa2 in mouse embryos and adult tissues. Gene Expr Patterns 2004; 5:193–208.
80. Gao Y, Bayless KJ, Li Q. TGFBR1 is required for mouse myometrial development. Mol Endocrinol 2014; 28:380–394.
81. Gao Y, Duran S, Lydon JP, DeMayo FJ, Burghardt RC, Bayless KJ, Bartholin L, Li Q. Constitutive activation of transforming growth factor Beta receptor 1 in the mouse uterus impairs uterine morphology and function. Biol Reprod 2015; 92:34.
82. Zhang Y, Xu X, Zhang M, Bai X, Li H, Kan L, Niu H, He P. ARID1A is downregulated in non-small cell lung cancer and regulates cell proliferation and apoptosis. Tumour Biol 2014; 35:5701–5707.
83. Wang XN, Das SK, Damm D, Klagsbrun M, Abraham JA, Dey SK. Differential regulation of heparin-binding epidermal growth factor-like growth factor in the adult ovariectomized mouse uterus by progesterone and estrogen. Endocrinology 1994; 135:1264–1271.
84. Shuya LL, Menkhorst EM, Yap J, Li P, Lane N, Dimitriadis E. Leukemia inhibitory factor enhances endometrial stromal cell decidualization in humans and mice. PLoS One 2011; 6:e25288.
85. Kawarabayashi Y, Hai L, Honda A, Horiuchi S, Tsujioka H, Ichikawa J, Inoue R. Critical role of TRPC1-mediated Ca(2)(+) entry in decidualization of human endometrial stromal cells. Mol Endocrinol 2012; 26: 846–858.
86. Kommagani R, Szwarc MM, Kovanci E, Creighton CJ, O'Malley BW, Demayo FJ, Lydon JP. A murine uterine transcriptome, responsive to steroid receptor coactivator-2, reveals transcription factor 23 as essential for decidualization of human endometrial stromal cells. Biol Reprod 2014; 90:75.
87. Li Q, Kannan A, Wang W, Demayo FJ, Taylor RN, Bagchi MK, Bagchi IC. Bone morphogenetic protein 2 functions via a conserved signaling pathway involving Wnt4 to regulate uterine decidualization in the mouse and the human. J Biol Chem 2007; 282:31725–31732.
88. Li Q, Kannan A, Das A, Demayo FJ, Hornsby PJ, Young SL, Taylor RN, Bagchi MK, Bagchi IC. WNT4 acts downstream of BMP2 and functions via beta-catenin signaling pathway to regulate human endometrial stromal cell differentiation. Endocrinology 2013; 154:446–457.
89. Aghajanova L, Hamilton A, Kwintkiewicz J, Vo KC, Giudice LC. Steroidogenic enzyme and key decidualization marker dysregulation in endometrial stromal cells from women with versus without endometriosis. Biol Reprod 2009; 80:105–114.
90. Peng J, Fullerton PT Jr, Monsivais D, Clementi C, Su GH, Matzuk MM. Uterine activin-like kinase 4 regulates trophoblast development during mouse placentation. Mol Endocrinol 2015; 29:1684–1693.
91. Peng J, Monsivais D, You R, Zhong H, Pangas SA, Matzuk MM. Uterine activin receptor-like kinase 5 is crucial for blastocyst implantation and placental development. Proc Natl Acad Sci U S A 2015; 112: E5098–E5107.
92. Sun X, Xie H, Yang J, Wang H, Bradshaw HB, Dey SK. Endocannabinoid signaling directs differentiation of trophoblast cell lineages and placentation. Proc Natl Acad Sci U S A 2010; 107: 16887–16892.
93. Cui Y, Wang W, Dong N, Lou J, Srinivasan DK, Cheng W, Huang X, Liu M, Fang C, Peng J, Chen S, Wu S, et al. Role of corin in trophoblast invasion and uterine spiral artery remodelling in pregnancy. Nature 2012; 484:246–250.
94. Lu J, Zhang S, Nakano H, Simmons DG, Wang S, Kong S, Wang Q, Shen L, Tu Z, Wang W, Wang B, Wang H, et al. A positive feedback loop involving Gcm1 and Fzd5 directs chorionic branching morphogenesis in the placenta. PLoS Biol 2013; 11:e1001536.
95. Kruse A, Martens N, Fernekorn U, Hallmann R, Butcher EC. Alterations in the expression of homing-associated molecules at the maternal/fetal interface during the course of pregnancy. Biol Reprod 2002; 66:333–345.
96. Kato S, Schwaederle M, Daniels GA, Piccioni D, Kesari S, Bazhenova L, Shimabukuro K, Parker BA, Fanta P, Kurzrock R. Cyclin-dependent kinase pathway aberrations in diverse malignancies: clinical and molecular characteristics. Cell Cycle 2015; 14:1252–1259.
97. Xie C, Fu L, Han Y, Li Q, Wang E. Decreased ARID1A expression facilitates cell proliferation and inhibits 5-fluorouracil-induced apoptosis in colorectal carcinoma. Tumour Biol 2014; 35:7921–7927.
98. Wang DD, Chen YB, Pan K, Wang W, Chen SP, Chen JG, Zhao JJ, Lv L, Pan QZ, Li YQ, Wang QJ, Huang LX, et al. Decreased expression of the ARID1A gene is associated with poor prognosis in primary gastric cancer. PLoS One 2012; 7:e40364.
99. Diaz-Gimeno P, Ruiz-Alonso M, Blesa D, Bosch N, Martinez-Conejero JA, Alama P, Garrido N, Pellicer A, Simon C. The accuracy and

reproducibility of the endometrial receptivity array is superior to histology as a diagnostic method for endometrial receptivity. Fertil Steril 2013; 99:508–517.
100. Garrido-Gomez T, Ruiz-Alonso M, Blesa D, Diaz-Gimeno P, Vilella F, Simon C. Profiling the gene signature of endometrial receptivity: clinical results. Fertil Steril 2013; 99:1078–1085.
101. Ruiz-Alonso M, Blesa D, Diaz-Gimeno P, Gomez E, Fernandez-Sanchez M, Carranza F, Carrera J, Vilella F, Pellicer A, Simon C. The endometrial receptivity array for diagnosis and personalized embryo transfer as a treatment for patients with repeated implantation failure. Fertil Steril 2013; 100:818–824.
102. Huang CC, Orvis GD, Wang Y, Behringer RR. Stromal-to-epithelial transition during postpartum endometrial regeneration. PLoS One 2012; 7:e44285.
103. Li XS, Trojer P, Matsumura T, Treisman JE, Tanese N. Mammalian SWI/SNF–a subunit BAF250/ARID1 is an E3 ubiquitin ligase that targets histone H2B. Mol Cell Biol 2010; 30:1673–1688.
104. Buza N, Xu F, Wu W, Carr RJ, Li P, Hui P. Recurrent chromosomal aberrations in intravenous leiomyomatosis of the uterus: high-resolution array comparative genomic hybridization study. Hum Pathol 2014; 45: 1885–1892.
105. Dallas PB, Pacchione S, Wilsker D, Bowrin V, Kobayashi R, Moran E. The human SWI-SNF complex protein p270 is an ARID family member with non-sequence-specific DNA binding activity. Mol Cell Biol 2000; 20:3137–3146.
106. Wilsker D, Patsialou A, Zumbrun SD, Kim S, Chen Y, Dallas PB, Moran E. The DNA-binding properties of the ARID-containing subunits of yeast and mammalian SWI/SNF complexes. Nucleic Acids Res 2004; 32: 1345–1353.
107. Nagl NG Jr, Zweitzig DR, Thimmapaya B, Beck GR Jr, Moran E. The c-myc gene is a direct target of mammalian SWI/SNF-related complexes during differentiation-associated cell cycle arrest. Cancer Res 2006; 66: 1289–1293.
108. Nagl NG Jr, Wang X, Patsialou A, Van Scoy M, Moran E. Distinct mammalian SWI/SNF chromatin remodeling complexes with opposing roles in cell-cycle control. EMBO J 2007; 26:752–763.
109. Kimura A, Arakawa N, Hirano H. Mass spectrometric analysis of the phosphorylation levels of the SWI/SNF chromatin remodeling/tumor suppressor proteins ARID1A and Brg1 in ovarian clear cell adenocarcinoma cell lines. J Proteome Res 2014; 13:4959–4969.
110. Kidder BL, Palmer S. Examination of transcriptional networks reveals an important role for TCFAP2C, SMARCA4, and EOMES in trophoblast stem cell maintenance. Genome Res 2010; 20:458–472.
111. Bai J, Mei P, Zhang C, Chen F, Li C, Pan Z, Liu H, Zheng J. BRG1 is a prognostic marker and potential therapeutic target in human breast cancer. PLoS One 2013; 8:e59772.